Theoretical analysis of optical injection locking in semiconductor DFB lasers, influence of the injection direction

Fabien Kéfélian and Philippe Gallion

École Nationale Supérieure des Télécommunications,
(GET/Télécom Paris & CNRS LTCI, UMR 5141 CNRS)
46 rue Barrault 75634, Paris, France

ABSTRACT

Theoretical results concerning injection locking in complex cavity semiconductor lasers are reported. A general equation for the complex temporal envelope of the optical field is derived. The injection direction influence is taken into account and the difference between front and rear phase noise is pointed out and demonstrated. Numerical results are given concerning the feed-in rate of different DFB lasers.

Keywords: Injection Locking, Semiconductor Laser, Phase Noise, DFB laser

1. INTRODUCTION

Injection locking is a particularly interesting method to reduce laser linewidth,[1] enhance the modulation bandwidth,[2] synchronize lasers for microwave generation[3],[4] or measure the linewidth enhancement factor.[5] Injection locking theoretical properties of lasers,[6] and especially semiconductor lasers,[7] were originally derived using analogies with the electrical and microwave oscillators[8] and especially from Adler's works on vacuum tube oscillator circuits.[9] Because microwave oscillators have only one input-output, the equation commonly used for optical injection locking[10] does not take into account the direction of the injection in comparison with the output field.

Injection locking in Fabry-Perot cavity semiconductor lasers has been the subject of a large number of papers,[11] but, although distributed feedback (DFB) lasers are among the most important industrial lasers used in optical telecommunications, the theoretical study of injection locking in DFB lasers or more complex structure cavity lasers has been the subject only of a few papers. Experimental studies have demonstrated that DFB lasers exhibit a symmetrical locking range[12] and a model based on a transfer function theory has been developed to determine the spectrum of an injected DFB laser.[13] To establish theoretical equations concerning optical injection into DFB semiconductor laser, we have adapted and developed previous works[14][15][16][17][18][19] concerning optical feedback and noise properties of complex structure cavity lasers based on transmission line theory and Green's function treatment of spontaneous emission.

2. FORWARD AND BACKWARD INJECTION: FIELD EQUATIONS

2.1. Introduction

We consider a laser of length l along the z axis. The laser is assumed to be spatially and spectrally single mode. It can be submitted to the optical injection of an other single mode laser through its right ($z = 0$) or left ($z = l$) facet. Only the output field emerging from the right facet is here considered. Consequently, the right facet is here referred as the front facet and the left facet as the rear facet.

Further authors informations: (Send correspondence to Fabien Kéfélian)
Fabien Kéfélian: E-mail: kefelian at enst.fr, Telephone: +33 (0)1 45 81 75 67
Philippe Gallion: E-mail: gallion at enst.fr, Telephone: +33 (0)1 45 81 77 02

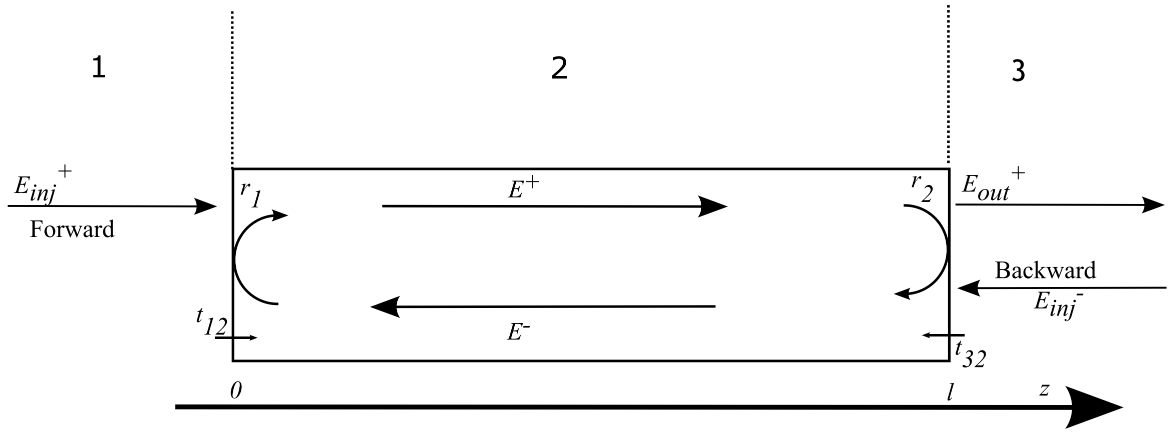

Figure 1. Forward and backward injection in a laser

2.2. Boundary equations for electrical field

The goal of this part is to establish an expression of the spectral components of the output electrical field.

The boundary conditions for spectral components of the input electrical fields at $z = 0$ and $z = l$ are the following ones:

$$E^+(0,\omega) = r_1 E^-(0,\omega) + t_{12} E^+_{inj}(0,\omega) \tag{1}$$

$$E^-(l,\omega) = r_2 E^+(l,\omega) + t_{32} E^-_{inj}(l,\omega) \tag{2}$$

where r_1 and r_2 are amplitude reflexion complex coefficients of the facets 1 and 2, and t_{12} and t_{32} are amplitude transmission complex coefficients, see Fig. 1.

In the transmission line theory,[20] the two input and two output fields are linked with the four coefficients of S matrix. We considered in this study only the output through the right facet ($z = l$), consequently, we use only two coefficients[14]:

$$E^+(l,\omega) = r_L E^-(l,\omega) + t_L E^+(0,\omega) \tag{3}$$

The effective transmission and reflexion coefficients t_L and r_L of the laser are functions of the laser structure (for example Bragg grating), of the optical frequency ω, of the internal loss and of the gain, i.e. of the spatial distribution of the densities of carriers $\mathcal{N}(z)$ and photons $\mathcal{P}(z)$, if the spatial and spectral hole burning is taken into account for the gain expression. Since r_L and t_L depend on the functions $\mathcal{N}(z)$ and $\mathcal{P}(z)$, they must be treated mathematically as functionals, i.e. functions of functions. Without spatial hole burning, they can be explicitly found in solving the propagation equations of the field, which form a linear system of coupled equations.

To take into account the spontaneous emission due to the quantification of the field,[21] a Langevin force F_L is included into the above expression[22]:

$$E^+(l,\omega) = r_L E^-(l,\omega) + t_L E^+(0,\omega) + F_L(\omega) \tag{4}$$

where

$$\langle F_L(\omega) F_L^*(\omega') \rangle = R_L \delta(\omega - \omega') \tag{5}$$

R_L can be determined using the Green's function method.[23] The expression of the right output field is established by the combination of the boundary equations (1), (2) and the transmission line equation (3):

$$E^+(l,\omega) = \frac{t_L t_{12} E^+_{inj}(0,\omega) + r_L t_{32} E^-_{inj}(l,\omega) + R_L}{1 - r_2 r_L} \tag{6}$$

The expression (6) exhibits three contributions to the output field: two come from the injected fields, corresponding to the amplification of an external signal, the last one comes from the spatially distributed spontaneous sources, corresponding to laser effect. Without injection, the lasing frequency corresponds to a value of the denominator closed from zero, i.e. from the resonance of the cavity.

The power spectral density of the output field can be established from the field expression (6) and the formal following relation relating the power spectral density of a random function X to its Fourier components $X(\omega)$: $S_X(\omega)\delta(\omega-\omega') = \langle X(\omega)X^*(\omega')\rangle$:

$$S_{E^+}(l,\omega) = \frac{|t_L t_{12}|^2 S_{E^+_{inj}}(0,\omega) + |r_L t_{32}|^2 S_{E^-_{inj}}(l,\omega) + R_L}{|1-r_2 r_L|^2} \tag{7}$$

2.3. Electrical field temporal envelope expression

To establish the expression of the complex temporal envelop of the right output electrical field, the functionals r_L and t_L are first order expended around the stationary solution $(\omega_s, \mathcal{N}_s, \mathcal{P}_s)$ of the solitary laser:

$$\frac{1}{r_L}(\omega,\mathcal{N},\mathcal{P}) = \left.\frac{1}{r_L}\right|_s + \frac{j}{f_R}(\omega-\omega_s) - \frac{1}{f_R}\left[\int_0^l C_{\mathcal{N}}(z)\Delta\mathcal{N}(z)dz + \int_0^l C_{\mathcal{P}}(z)\Delta\mathcal{P}(z)dz\right] \tag{8}$$

$$\frac{t_L}{r_L}(\omega,\mathcal{N},\mathcal{P}) = \left.\frac{t_L}{r_L}\right|_s \left[1 + \frac{j\chi_t}{f_T}(\omega-\omega_s) + \frac{1}{f_T}\left[\int_0^l C^t_{\mathcal{N}}(z)\Delta\mathcal{N}(z)dz + \int_0^l C^t_{\mathcal{P}}(z)\Delta\mathcal{P}(z)dz\right]\right] \tag{9}$$

f_R is called the feed-in rate for backward injection, i.e. injection through the output facet, it is inversely proportional to a generalized round trip time, $C_{\mathcal{N}}$ is the local differential gain for a round trip, $C_{\mathcal{P}}$ is a local parameter taking into account gain compression, $C^t_{\mathcal{N}}$, $C^t_{\mathcal{P}}$ are similar factors for a single trip, $\Delta\mathcal{N}(z)$ and $\Delta\mathcal{P}(z)$ are the local deviations from the carrier and photon densities without injection. f_T is the feed-in rate for forward injection, i.e. injection through the rear facet, χ_t is a dimensionless factor taking into account experimented trip difference between front emerging and injected waves in forward injection.

The temporal envelop of the electrical fields around the master angular frequency ω_m are hereunder defined:

$$A^+(t) = \frac{1}{2\pi}\int_0^\infty E^+(l,\omega)e^{j(\omega-\omega_m)}d\omega \tag{10}$$

$$A^+_{inj}(t) = \frac{1}{2\pi}\int_0^\infty E^+_{inj}(0,\omega)e^{j(\omega-\omega_m)}d\omega \tag{11}$$

$$A^-_{inj}(t) = \frac{1}{2\pi}\int_0^\infty E^-_{inj}(l,\omega)e^{j(\omega-\omega_m)}d\omega \tag{12}$$

$A^+(t)$ is the temporal envelope of the electrical field at the $z=l^-$ output of the laser, $A^-_m(t)$ and $A^+_m(t)$ are the temporal envelopes of the electrical injected fields respectively through the front facet ($z=l^-$) and rear facet ($z=0^+$), see Fig. 1.

The differential evolution equation of the output field temporal envelop for forward and backward injections are established using Fourier transform of the equation (6) with the first order expensions (8) and (9):

$$\frac{dA^+}{dt}(t) = j(\omega_m-\omega_0)A^+(t) + \int_0^l \left[C_{\mathcal{N}}(z)\Delta\mathcal{N}(z,t) + C_{\mathcal{P}}(z)\Delta\mathcal{P}(z,t)\right]dzA^+(t) + f_R t_{32}A^-_m(t) + F_A(t) \tag{13}$$

$$\begin{aligned}\frac{dA^+}{dt}(t) = {} & j(\omega_m-\omega_0)\left[A^+(t) + \chi_t t_{12}A^+_m(t)\right] + \int_0^l \left[C_{\mathcal{N}}(z)\Delta\mathcal{N}(z,t) + C_{\mathcal{P}}(z)\Delta\mathcal{P}(z,t)\right]dzA^+(t) \\ & + f_T t_{12}A^+_m(t) + \int_0^l \left[C^t_{\mathcal{N}}(z)\Delta\mathcal{N}(z,t) + C^t_{\mathcal{P}}(z)\Delta\mathcal{P}(z,t)\right]dz t_{12}A^+_m(t) + \chi_t t_{12}\frac{dA^+_m}{dt} + F_A(t)\end{aligned} \tag{14}$$

For backward injection (13), the variation of the temporal envelop is composed of five contributions. The first is the rotation of the complex envelop due to the detuning of the field with respect to the laser cavity, the second term takes into account the double effect of the carrier density deviation from its free-running value: firstly the gain change, corresponding to the real part of $C_{\mathcal{N}}$ and inducing a modification of the amplitude, and secondly the change of the refractive index, corresponding to the imaginary part of $C_{\mathcal{N}}$, which induces an additional rotation of the field envelop. The third term takes into account the non-linear gain effect on the photon density deviation from its free-running value. The fourth term is the contribution of the injected field which is determined by the feed-in rate f_R, the fifth $F_A(t)$ is the Langevin force taking into account distributed spontaneous emission inside the laser.[23]

The equation (14), corresponding to the forward injection, exhibits three additional contributions. These ones are due to the field modification in a single path amplification into the cavity. χ_t is a key parameter for these contributions.

Whereas backward injection equation (13) is a generalized form of the commonly used equation[10] taken into account spatial and spectral hole burning, forward injection equation (14) exhibits new additional contributions among them one from the injected signal derivate, specific to the injection through the rear facet.

3. NUMERICAL RESULTS ON FEED-IN RATE OF DFB LASERS

3.1. Introduction

The feed-in rate is an essential parameter of the locking range expression. In lots of papers[2410252627,28] this parameter is empirically determined to be equal to the free spectral range. In fact, our analysis shows that the feed-in rate is strongly dependent on the reflectivity of the facets. Indeed, the feed-in rates can be determined using the Fabry-Perot expression of the effective reflectivity:

$$r_L = r_1 exp\left[-j2\left(\frac{\omega}{c}n\left(\omega,\mathcal{N}\right)+\frac{j}{2}g\left(\omega,\mathcal{N}\right)\right)\right] \tag{15}$$

where n is the refractive index and g the net modal gain, and the partial first order developments (8) and (9) versus the frequency, given:

$$f_R = \frac{1}{r_2}\frac{v_g}{2l} \tag{16}$$

$$f_T = \frac{1}{\sqrt{r_1 r_2}}\frac{v_g}{2l} \tag{17}$$

with v_g the group velocity. For a cleaved facet Fabry-Perot laser, the feed-in factor for both directions is 1.8 time the free spectral range.

3.2. Influence of the grating coupling factor

We have represented on Fig. 2 the module of the feed-in rate of a DFB laser with an anti-reflection coated output right facet, for different real values of the opposite facet reflectivity, in function of the normalized grating coupling factor $\kappa.l$. The feed-in rates f_R or f_T are normalized by the free spectral range $1/\tau_{in}$ of the Fabry-Perot cavity with the same length, τ_{in} is the group round trip time. The backward case corresponds to an injection through the anti-reflexion coated facet, whereas the forward case corresponds to the injection through the facet with the reflectivity r_1. Consequently, for the forward case, the feed-in rate as defined above takes into account only the effect of the internal cavity and must be multiplied by the transmission factor to obtain the effective coupling factor to the external field.

At first sight, for both cases, the feed-in rate decreases with an increase of the grating coupling rate. Indeed, for a Fabry-Perot cavity, the reflections are localized at both facets whereas for a DFB cavity, additional reflections are localized inside the cavity due to the Bragg grating. With a very high grating coupling factor, most of the round trips are localized inside the grating and are not coupled to the external field. On the other hand, when

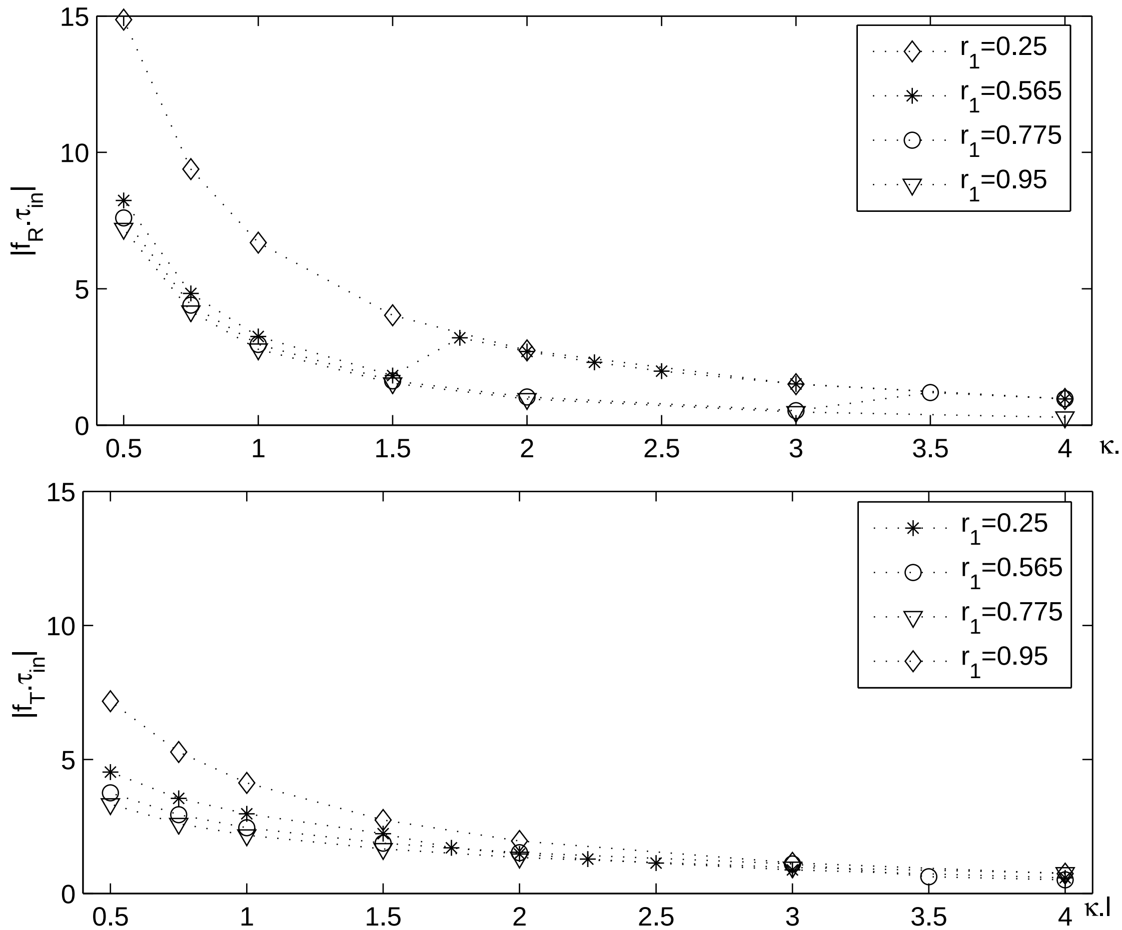

Figure 2. Feed-in rate for backward and forward injection in function of the grating coupling factor for different reflectivity values of the left facet

the coupling to the grating is weak, the feed-in rate becomes very high since the output facet is anti-reflection coated.

In the backward case, the values for different reflectivities are localized on two curved bands. The switch from one to the other with the grating coupling factor corresponds to a mode hopping with a change of the sign of the detuning in comparison with the Bragg mode. Consequently, although the injection is performed through the anti-reflexion coated facet, the influence of the opposite facet reflectivity is obvious. Moreover, the mode hopping occurring with an increase of the grating coupling factor results in an increase of the feed-in rate, which is a correction to the behavior previously explained.

In the forward case, the effect of the mode hopping is inverse. Indeed, the feed-in rate becomes lower when a mode hopping occurs with an increase of the grating coupling factor, but the values are not arranged around two curves, because the facet of injection is the facet whose reflectivity is modified.

The value of the feed-in rate for a Fabry-Perot cavity laser with cleaved facet being $f_R = 1.8/\tau_{in}$, consequently, for the backward configuration, a DFB laser with a $\kappa.l > 2.5$ is less sensitive to the injection than a cleaved cavity Fabry-Perot laser, whereas it is more sensitive for $\kappa.l < 1.5$.

3.3. Influence of the reflectivity phase

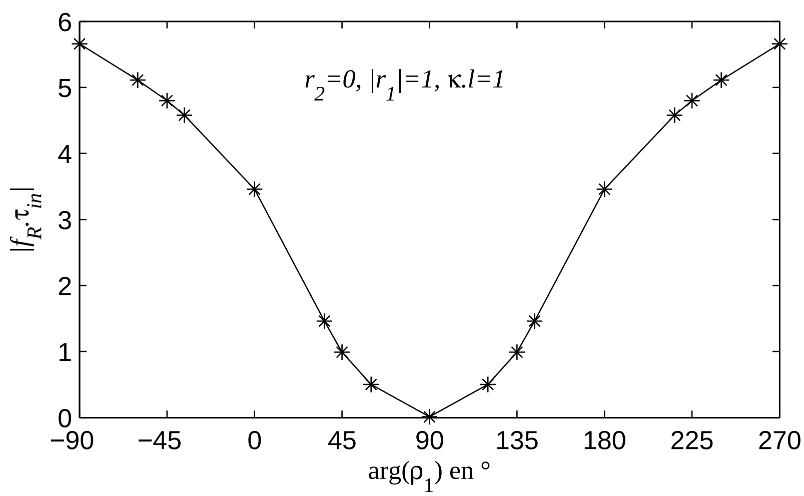

Figure 3. Feed-in rate for backward injection in function of the rear facet phase for a AR/HR DFB laser

It is well known that DFB spectral properties are strongly dependent on the phase and the reflectivity of their facets. We have numerically studied the case of a DFB laser with an anti-reflexion (AR) coated front facet and a high reflexion (HR) coating on the rear facet, with an arbitrary phase. We have represented on Fig. 3 the computed values of the feed-in rate, for backward injection, in function of the argument of the complex amplitude reflectivity of the rear facet. It appears that for a purely imaginary rear reflectivity, i.e. a phase shift of $\lambda/4$, the feed-in rate is closed from zero and the variation of the feed-in rate for values of the argument in the neighborhood of $\pi/2$ is strong. Consequently, the locking range for a purely imaginary facet with high reflectivity is extremely small.

3.4. Influence of the reflectivity module

On Fig. 4 is represented the influence of the module of the reflectivity on the feed-in rate in backward injection, for a $\pi/2$ argument, i.e. for a DFB laser with its laser mode in the gap band.[29] The curves show a large range of values, we can notice that for high rear reflectivities, the normalized feed-in rate is below unity, but for low values of the rear reflectivity, the feed-in rate can reach very high values, corresponding to very wide locking ranges.

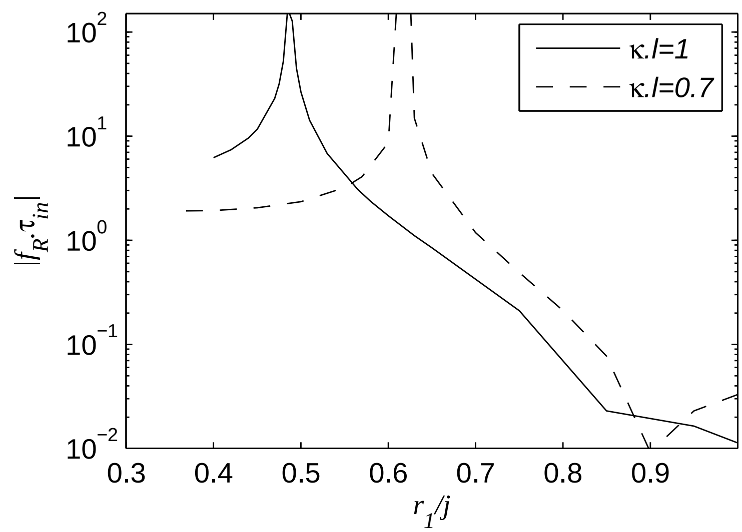

Figure 4. Feed-in rate for backward injection in function of the rear facet reflectivity for gap mode DFB laser

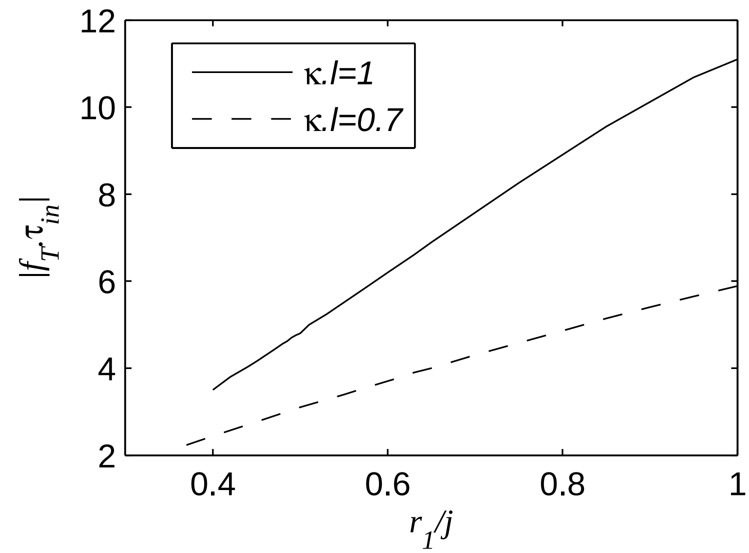

Figure 5. Feed-in rate for forward injection in function of the rear facet reflectivity for gap mode DFB laser

The feed-in rate for forward injection is now considered. Computed values are presented on Fig. 5 in function of the absolute value of the rear amplitude reflectivity. The curves show a behavior different from the backward injection case. In particular, the range of values taken by the feed-in rate are limited, moreover, when the transmission of the facet of injection, i.e. the rear facet, is taken into account, the effective feed-in rate values are, for $\kappa.l = 1$, between 0 and 4.

4. PHASE NOISE OF INJECTION LOCKED LASER

4.1. Equations and analysis

Injection locking is a well-known technique to narrow the spectral lineshape of a powerful laser using a highly stable low power master laser. This technique is based on the phase noise proprieties of the injection locked laser. Phase equation is derived from equations (13) and (14) in separating real and imaginary parts. After calculations, two differential equations are obtained for the phase of the slave laser, one for the backward injection (18) and one for the forward injection (19):

$$\begin{aligned} \frac{d\phi}{dt}(t) &= (\omega_s - \omega_i) + \langle C_{\mathcal{N}i} \,|\Delta\mathcal{N}(t)\rangle + \langle C_{\mathcal{P}i} \,|\Delta\mathcal{P}(t)\rangle \\ &\quad + |f_R|\, T_2 \sqrt{\frac{I_{in}(t)}{I(t)}} \left[\sin(\phi_{in}(t) - \phi(t) + \arg\{t_{32} f_R\})\right] + F_\phi(t) \end{aligned} \tag{18}$$

$$\begin{aligned} \frac{d\phi}{dt}(t) &= (\omega_s - \omega_i) + \left[\langle C_{\mathcal{N}i}|\, \Delta\mathcal{N}(t)\rangle + \langle C_{\mathcal{P}i}|\, \Delta\mathcal{P}(t)\rangle\right] \\ &\quad + |f_T| \sqrt{T_1 T_2} \sqrt{\frac{I_{in}(t)}{I(t)}} \sin(\phi_{in}(t) - \phi(t) + \arg\{f_T t_{12}\}) \\ &\quad + \left|\langle C^t_{\mathcal{N}}|\, \Delta\mathcal{N}(t)\rangle + \langle C^t_{\mathcal{P}}|\, \Delta\mathcal{P}(t)\rangle\right| \sqrt{T_1 T_2} \sqrt{\frac{I_{in}(t)}{I(t)}} \\ &\qquad \times \sin\left(\phi_{in}(t) - \phi(t) + \arg\left\{t_{12} \langle C^t_{\mathcal{N}}|\, \Delta\mathcal{N}(t)\rangle + \langle C^t_{\mathcal{P}}|\, \Delta\mathcal{P}(t)\rangle\right\}\right) \\ &\quad + |\chi_t|\, (\omega_i - \omega_s) \sqrt{T_1 T_2} \sqrt{\frac{I_{in}(t)}{I(t)}} \cos\left(\phi_{in}(t) - \phi(t) + \arg\{\chi_t t_{12}\}\right) \\ &\quad + \frac{1}{2} |\chi_t| \frac{dI_{in}}{dt}(t) \sqrt{T_1 T_2} \sqrt{\frac{1}{I_{in}(t) I(t)}} \sin\left(\phi_{in}(t) - \phi(t) + \arg\{\chi_t t_{12}\}\right) \\ &\quad + |\chi_t| \frac{d\phi_{in}}{dt}(t) \sqrt{T_1 T_2} \sqrt{\frac{I_{in}(t)}{I(t)}} \cos\left(\phi_{in}(t) - \phi(t) + \arg\{\chi_t t_{12}\}\right) \\ &\quad + F_\phi(t) \end{aligned} \tag{19}$$

where we have used the notation:

$$\langle f|\, g\rangle = \int_0^l f(z) g(z) dz \tag{20}$$

$C_{\mathcal{N}i}$ and $C_{\mathcal{P}i}$ are imaginary parts of respectively $C_{\mathcal{N}}$ and $C_{\mathcal{P}}$. T_1 and T_2 are the intensity transmission coefficients of the facet respectively 1 and 2. $I(t)$ is the optical power emerging out of the laser through the right facet, $I_{in}(t)$ is the optical power enlightening the right facet (backward case) or the left facet (forward case). They are proportional respectively to $|A^+(t)|^2$, $|A^+_{inj}(t)|^2$ or $|A^-_{inj}(t)|^2$. The imaginary part of $C_{\mathcal{P}}$ corresponds to a modification of the refraction index induced by a modification of the photon density, and can be neglected most of the time.

As above-mentioned, the backward case corresponds to a generalization of the case commonly studied with Fabry-Perot cavity. The variation of the phase is the sum of four contributions: the detuning in comparison with the unlocked cavity resonance frequency, the refractive index modification of the cavity induced by carrier density modification, the injected field contribution depending on the difference between the master phase and the slave phase, and a Langevin force representing the direct contribution of the spontaneous emission to the phase evolution.

The equation corresponding to the forward injection exhibits four additional contributions to the phase evolution. The first one involves the carrier and photon densities deviation from the free-running values, the second one involves the detuning, the third one involves the master power variation and the fourth one involves the master phase variation. The two last mentioned contributions have no influence on the locking range but have one on the stability of the locking. Moreover, they have important impact on the phase noise spectral proprieties of the locked laser.

4.2. Transfer of noise

The usual noise equations of injection locked lasers[27] correspond to the backward injection. In this case, the phase noise transfer from the master laser to the slave laser acts as a second order low pass filter with a cut frequency proportional to the feed-in rate f_R. That means that the very fast fluctuations of the master phase cannot be transmitted to the slave laser and consequently there is a large amount of remaining free phase noise in the high frequencies part of the phase noise spectrum. However, for the forward injection, the phase noise equation involves not only the master phase noise but also its first derivate. Consequently, in forward configuration, the phase noise spectral components of the master laser field can be transferred even for large noise frequencies, thanks to the resonance of the cavity. This effect depends on the above-mentioned χ_t factor and appears to be stronger in cleaved facet Fabry-Perot laser ($\chi = 0.9$) than in anti-reflexion coated single facet DFB laser, see Fig. 6, where it can be canceled with a specific reflectivity value depending on the grating coupling coefficient, moreover, it is stronger in long cavity i.e. short free spectral range.

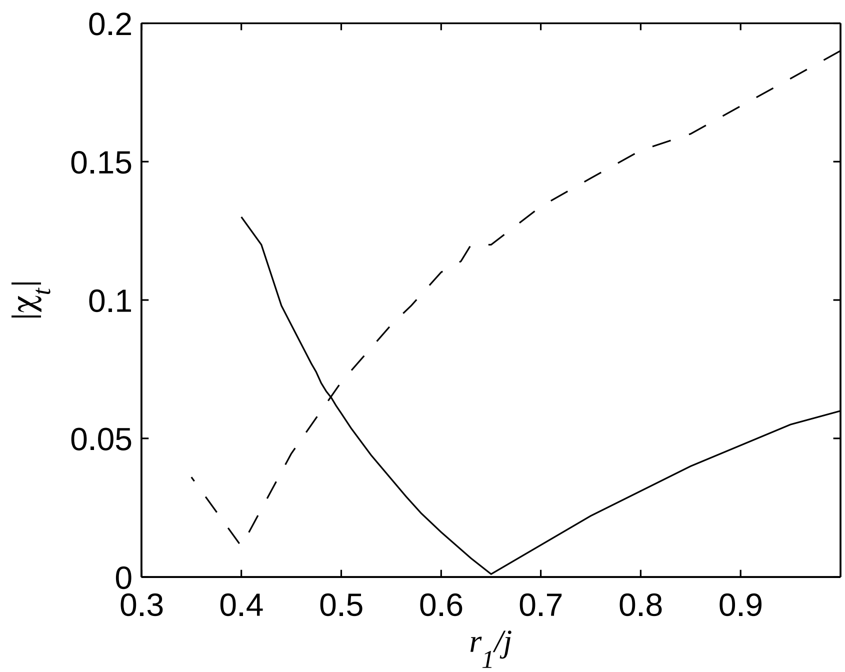

Figure 6. Module of χ_t parameter for forward injection in function of the rear facet reflectivity for gap mode DFB laser

4.3. Noise asymmetry

Until now we have considered the output field through the right facet, and injection through right and left facets. Now if we consider injection through the right facet and output through the right and left facets, we obtain that the phase equation is different for each output field. Consequently, a perfectly symmetric laser submitted to external light injection exhibits a different noise spectrum at each output.

5. CONCLUSIONS

Using a transmission line and Green's function approach with electromagnetic boundary conditions, taking into account field injection through each side, we have derived, for the first time to our knowledge, theoretical general equations for the laser field of a complex cavity laser, such as DFB or DBR lasers, submitted to coherent optical injection by output side facet (backward) or opposite side facet (forward). These equations take into account spatial hole burning and gain compression, but fundamental results also appears in low power Fabry-Perot laser. We have given numerical results for different parameters of a DFB laser. The differential equation of the phase has been determined for both directions of injection and particular effects concerning phase noise transfer have been outlined.

REFERENCES

1. F. Mogensen, H. Olesen, and G. Jacobsen, "FM noise suppression and linewidth reduction in an injection-locked semiconductor laser," *Electronics Letters* **21**(16), pp. 696–697, 1985.
2. O. Lidoyne, P. B. Gallion, and D. Erasme, "Modulation properties of an injection-locked semiconductor laser," *IEEE Journal of Quantum Electronics* **27**(3), pp. 344 –351, 1991.
3. K. Kikuchi, C.-E. Zah, and T. Lee, "Amplitude-modulation sideband injection locking characteristics of semiconductor lasers and their application," *Journal of Lightwave Technology* **6**(12), pp. 1821–1830, 1988.
4. L. Goldberg, H. F. Taylor, J. F. Weller, and D. M. Bloom, "Microwave generation with injection-locked laser diodes," *Electronics Letters* **19**, pp. 491–493, 1983.
5. R. Hui, A. Mecozzi, A. d'Ottavi, and P. Spano, "Novel measurement technique of α factor in DFB semiconductor lasers by injection locking," *Electronics Letters* **26**(14), pp. 997–998, 1990.
6. C. J. Buczek, R. J. Freiberg, and M. L. Skolnick, "Laser injection locking," *Proceedings of the IEEE* **61**(10), pp. 1411–1431, 1973.
7. S. Kobayashi and T. Kimura, "Injection locking in AlGaAs semiconductor laser," *IEEE Journal of Quantum Electronics* **17**(5), pp. 681–689, 1981.
8. K. Kurokawa, "Injection locking of microwave solid-state oscillators," *Proceedings of the IEEE* **61**(10), pp. 1386–1410, 1973.
9. R. Adler, "A study of locking phenomena in oscillators," in *Proceedings IRE*, **34**, pp. 351–356, 1946.
10. R. Lang, "Injection locking properties of a semiconductor laser," *IEEE Journal of Quantum Electronics* **18**(6), pp. 976 –983, 1982.
11. G. H. M. van Tartwijk and D. Lenstra, "Semiconductor lasers with optical injection and feedback," *Quantum and Semiclassical Optics* **7**(2), pp. 87–143, 1995.
12. R. Hui, A. D'Ottavi, A. Mecozzi, and P. Spano, "Injection locking in distributed feedback semiconductor lasers," *IEEE Journal of Quantum Electronics* **27**(6), pp. 1688–1695, 1991.
13. G. M. Stéphan, P. Besnard, M. Bondiou, R. Gabet, and M. Têtu, "Properties of a distributed feedback semiconductor laser submitted to optical injection," in *Proceedings of SPIE*, **3862**, pp. 28–37, 1999.
14. B. Tromborg, H. Olesen, X. Pan, and S. Saito, "Transmission line description of optical feedback and injection locking for Fabry-Perot and DFB lasers," *IEEE Journal of Quantum Electronics* **23**(11), pp. 1875 – 1889, 1987.
15. B. Tromborg and J. Mø rk, "Nonlinear injection locking dynamics and the onset of coherence collapse in external cavity lasers," *IEEE Journal of Quantum Electronics* **26**(4), pp. 642–654, 1990.
16. G.-H. Duan, P. Gallion, and G. Debarge, "Analysis of the phase-amplitude coupling factor and spectral linewidth of distributed feedback and composite-cavity semiconductor lasers," *IEEE Journal of Quantum Electronics* **26**(1), pp. 32–44, 1990.
17. B. Tromborg, H. Olesen, and X. Pan, "Theory of linewidth for multielectrode laser diodes with spatially distributed noise sources," *IEEE Journal of Quantum Electronics* **27**(2), pp. 178–192, 1991.
18. H. Olesen, B. Tromborg, X. Pan, and H. E. Lassen, "Stability and dynamic properties of multi-electrode laser diodes using Green's function approach," *IEEE Journal of Quantum Electronics* **29**(8), pp. 2282–2301, 1993.

19. F. Grillot, B. Thedrez, and G.-H. Duan, "Feedback sensitivity and coherence collapse threshold of semiconductor dfb lasers with complex structures," *IEEE Journal of Quantum Electronics* **40**(3), pp. 231 – 240, 2004.
20. T. Makino, "Transfer-matrix analysis of the intensity and phase noise of multisection DFB semiconductor lasers," *IEEE Journal of Quantum Electronics* **27**(11), pp. 2404–2414, 1991.
21. C. Henry and R. F. Kazarinov, "Quantum noise in photonics," *Review of Modern Physics* **68**(3), pp. 802 – 851, 1996.
22. M. Lax, "Classical noise IV:Langevin methods," *Review of Modern Physics* **38**, pp. 541–566, 1966.
23. C. H. Henry, "Theory of spontaneous emission noise in open resonators and its application to lasers and optical amplifiers," *Journal of Lightwave Technology* **4**(3), pp. 288–297, 1986.
24. K. Otsuka and S. Tarucha, "Theoretical studies on injection locking and injection-induced modulation of laser diodes," *IEEE Journal of Quantum Electronics* **17**(8), pp. 1515–1521, 1981.
25. F. Mogensen, H. Olesen, and G. Jacobsen, "Locking conditions and stability properties for a semiconductor laser with external light injection," *IEEE Journal of Quantum Electronics* **21**(7), pp. 784–793, 1985.
26. C. H. Henry, N. A. Olsson, and N. K. Dutta, "Locking range and stability of injection locked 1.54 μm InGaAsP," *IEEE Journal of Quantum Electronics* **21**(8), pp. 1152–1156, 1985.
27. P. Spano, S. Piazzolla, and M. Tamburrini, "Frequency and intensity noise in injection-locked semiconductor lasers: theory and experiments," *IEEE Journal of Quantum Electronics* **22**(3), pp. 427–435, 1986.
28. O. Lidoyne, P. Gallion, C. Chabran, and G. Debarge, "Locking range, phase noise and power spectrum of an injection-locked semiconductor laser," *IEE Proceedings* **137**(J3), pp. 147 –154, 1990.
29. C. H. Henry, "Performance of distributed feedback lasers designed to favor the energy gap model," *IEEE Journal of Quantum Electronics* **21**(12), pp. 1913–1918, 1985.